



ISTITUTO NAZIONALE DI RICERCA METROLOGICA  
Repository Istituzionale

Effect of mechanical cutting on the energy loss of laser-scribed grain-oriented alloys

This is the author's accepted version of the contribution published as:

*Original*

Effect of mechanical cutting on the energy loss of laser-scribed grain-oriented alloys / Manescu (Paltanea), V., Paltanea, G., Ferrara, E., Nemoianu, I.V., Fiorillo, F., Gavrilă, H.. - In: JOURNAL OF MAGNETISM AND MAGNETIC MATERIALS. - ISSN 0304-8853. - 565:(2023), p. 170212. [10.1016/j.jmmm.2022.170212]

*Availability:*

This version is available at: 11696/75519 since: 2024-01-27T06:44:41Z

*Publisher:*

Elsevier

*Published*

DOI:10.1016/j.jmmm.2022.170212

*Terms of use:*

This article is made available under terms and conditions as specified in the corresponding bibliographic description in the repository

*Publisher copyright*

(Article begins on next page)

## Journal Pre-proofs

Effect of mechanical cutting on the energy loss of laser-scribed grain-oriented alloys

Veronica Manescu(Paltanea), Gheorghe Paltanea, Enzo Ferrara, Iosif Vasile Nemoianu, Fausto Fiorillo, Horia Gavrilă

PII: S0304-8853(22)01097-6  
DOI: <https://doi.org/10.1016/j.jmmm.2022.170212>  
Reference: MAGMA 170212

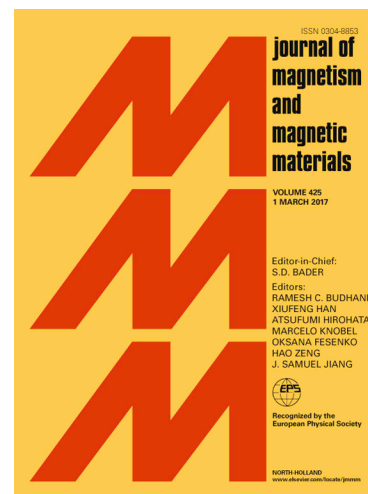
To appear in: *Journal of Magnetism and Magnetic Materials*

Received Date: 17 May 2022  
Revised Date: 22 September 2022  
Accepted Date: 18 November 2022

Please cite this article as: V. Manescu,(Paltanea) G. Paltanea, E. Ferrara, I. Vasile Nemoianu, F. Fiorillo, H. Gavrilă, Effect of mechanical cutting on the energy loss of laser-scribed grain-oriented alloys, *Journal of Magnetism and Magnetic Materials* (2022), doi: <https://doi.org/10.1016/j.jmmm.2022.170212>

This is a PDF file of an article that has undergone enhancements after acceptance, such as the addition of a cover page and metadata, and formatting for readability, but it is not yet the definitive version of record. This version will undergo additional copyediting, typesetting and review before it is published in its final form, but we are providing this version to give early visibility of the article. Please note that, during the production process, errors may be discovered which could affect the content, and all legal disclaimers that apply to the journal pertain.

© 2022 Elsevier B.V. All rights reserved.



Veronica Manescu (Paltanea)<sup>a,b</sup>, Gheorghe Paltanea<sup>a,\*</sup>, Enzo Ferrara<sup>c</sup>, Iosif Vasile Nemoianu<sup>a</sup>,  
Fausto Fiorillo<sup>c</sup>, Horia Gavrila<sup>a</sup>

<sup>a</sup> *University Politehnica of Bucharest, Faculty of Electrical Engineering, Bucharest, RO 060042, Romania,  
gheorghe.paltanea@upb.ro, paltanea03@yahoo.com*

<sup>b</sup> *University Politehnica of Bucharest, Faculty of Material Science and Engineering,  
Bucharest, RO-060042, Romania*

<sup>c</sup> *Advanced Materials Metrology and Life Sciences, Istituto Nazionale di Ricerca Metrologica—INRIM, 10135 Torino, Italy*

*Keywords: Energy loss, grain-oriented Fe-Si, strain-hardening, sheet cutting, Epstein strips.*

## Abstract

We investigate the effect of mechanical cutting on the magnetic properties of high permeability grain-oriented (HGO) laser-scribed Fe-Si sheets. Measurements have been performed on strips of different widths (5 to 60 mm) cut from 0.27 mm thick sheets. Normal magnetization curve and energy loss have been determined by means of a digitally controlled single strip tester from 1 Hz to 1 kHz at peak magnetic polarization values  $J_p = 1000$  mT and 1700 mT. The results fit into a simple phenomenological model regarding the dependence of magnetization curve and energy loss on the strip width, in substantial continuity with the approach originally developed for non-oriented electrical steels. The hysteresis  $W_h$  and excess  $W_{exc}$  loss components are shown to depend on the strip width according to a hyperbolic law, with a limiting fully hardened strip predicted to occur for widths around 3.5 mm. It is then consistently observed that the mechanical cutting of standard 30 mm wide HGO Epstein strips is conducive to an increase of the energy loss at 50 Hz and 1.7 T of the order of 13 %.

## 1. Introduction

High-permeability grain-oriented (HGO) Fe-Si sheets are endowed with sharp directional texture and widely spaced domain walls. Consequently, they display excellent quasi-static magnetic behavior, but, because of the largely inhomogeneous magnetization process, the dynamic losses can increase. For this reason, laser scribing of the sheets, a non-contact technique smoothly incorporated in the production process, is applied to top-quality industrial products, in order to achieve, by a combination of local magnetostatic and magnetoelastic effects, a refinement of the domain structure [1, 2]. This treatment conveniently leads to a substantial decrease of the excess loss component  $W_{exc}$ , at the cost of a slightly increased quasi-static loss  $W_h$  [3, 4].

Sheet cutting, as required for the assemblage of the transformer cores, can partially impair, however, the excellent magnetic properties of these materials at the working frequencies. It is an effect descending from the residual stress induced by cutting along the strip edges and the ensuing additional magnetoelastic energy. A further complication arises with standard magnetic characterization of laser-scribed sheets by the Epstein method. In this case, scribing must be done on the cut Epstein strips after a stress-relief treatment, a cumbersome operation. On the other hand, there is no universal acceptance for the standard Single Sheet Test method (500 mm  $\times$  500 mm sheet) [5], while the suggested use of 100 mm wide strips in a giant Epstein frame is at the laboratory stage [6].

It is therefore important to know the extent to which the mandatory cutting operations deteriorate the dc and ac magnetic properties of the high-permeability GO sheets. Typical literature approaches look at the problem either from the viewpoint of quasi-static hysteresis modeling or of loss modeling by extensive use of numerical techniques [7–12], making the whole matter a quite complex affair. We have thus proposed in recent times a simple phenomenological model of the loss dependence on the width of non-oriented Fe-Si strips, obtained by guillotine punching and water cutting, based on the concept of loss separation [13, 14, 15]. Besides putting in evidence the extent to which  $W_h$  and  $W_{exc}$  are separately affected by the cutting operation, an estimate for the breadth of the strain-hardened region at the sample

edges is made available. We show in the following that the very same physical concepts can be usefully applied to quantify the extent to which the punching operation can affect the magnetic losses of HGO Fe-Si sheets across a broad range of frequencies, up to 1kHz.

## 2. Materials and methods

Guillotine-punched strips of HGO laser-scribed Power Core-H-095-27, cut from a 0.27 mm thick parent sheet by a Krass Q11-2X2500 shearing machine, have been investigated. The clearance of the shearing machine was set at 35  $\mu$ m, with punch radius 30 to 45  $\mu$ m and surface pressure under the blank holder of 300 MPa.

300 mm long strips of width ranging between 5 mm and 60 mm were cut along the rolling direction (RD). They were characterized by means of a single sheet tester in the frequency range  $1 \text{ Hz} \leq f \leq 1 \text{ kHz}$  at the peak magnetic polarization values  $J_p = 1.0$  T and 1.7 T. A calibrated hysteresisgraph-wattmeter endowed with digital control of the sinusoidal induction waveform was used, where the magnetizing current is supplied by combination of an Agilent 33220 arbitrary function generator and a dc-coupled NF HSA4101 power amplifier, whereas signal acquisition and conversion are achieved by means of a 12-bit 500 MHz HDO4045 LeCroy oscilloscope.

The strips were placed side-by-side between the 120 mm  $\times$  30 mm pole faces of double-C laminated yoke, to form, whatever the strip width, a 60 mm wide sheet sample. The number of simultaneously tested strips accordingly ranged from 1 to 12. A constant magnetic path length of  $l_m = 240$  mm, equal to the distance between the pole faces, was assumed in all cases.

The energy loss versus frequency behaviors were analyzed by identification of the hysteresis  $W_h$ , excess  $W_{exc}$ , and classical  $W_{cl}$  loss components [16, 17, 18].  $W_h$  is obtained by extrapolating the measured loss to  $f = 0$ , while  $W_{cl}$  is calculated according to standard formulations [19], where a defined DC permeability value is assigned to the material for any  $J_p$  value. The skin effect, appearing beyond about 400 Hz, is in this way only approximately accounted for in the upper frequency range.

### 3.1. Normal magnetization curve

The normal magnetization curve, measured up to the maximum field value  $H_{\max} = 5500$  A/m, shows the expected deterioration of the soft magnetic behavior engendered by cutting, which extends across the whole 0.02 to 1.95 T tested  $J_p$  interval. This is illustrated in Fig. 1 by the monotonical decrease of the material permeability upon the decrease of the strip width from 60 to 5 mm. This response is somewhat magnified with respect to the effect observed in non-oriented Fe-Si sheets. A same modeling scheme is here applied, where the cut sample of width  $w$  is described as made of an undamaged core region and two strain-hardened lateral strips of equal width  $L_c$  [13, 14, 17] (inset in Fig. 1). If  $J_p$  is the experimentally measured peak magnetic polarization, and  $J_{pc}$  and  $J_{p0}$  are the peak magnetic polarizations in the damaged ( $2L_c$  wide) and undamaged ( $w - 2L_c$  wide) longitudinal slabs, respectively, it follows from our scheme that these quantities are related by the equation

$$J_p(w) = J_{p0} - (J_{p0} - J_{pc}) \frac{2L_c}{w}, \quad (w \geq 2L_c) \quad (1)$$

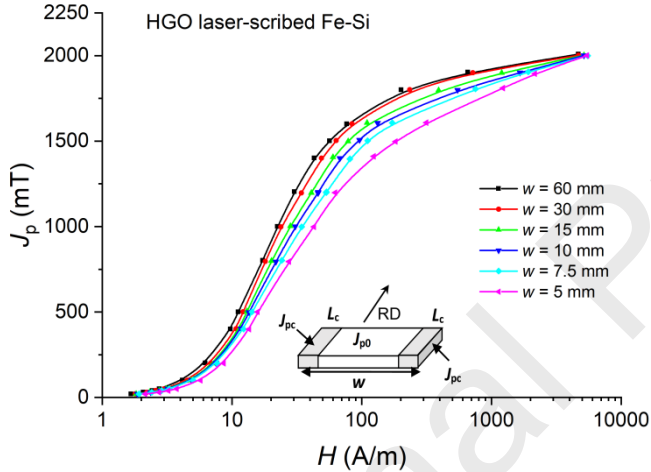


Fig. 1. Quasi-static normal magnetization curves versus width  $w$  of the punched strip samples (0.27 mm thick HGO Fe-Si strips).

We consider Eq. (1) for a defined applied field  $H$  and write it as  $J_p(w, H) = J_{p0}(H) - a(H)/w$ , where we denote, in short,  $a(H) = (J_{p0}(H) - J_{pc}(H)) \cdot 2L_c$ . By taking two experimental reference  $J(H)$  curves, taken on conveniently wide strips (for example,  $w_1 = 10$  mm,  $w_2 = 30$  mm in Fig. 1), the two quantities  $J_{p0}(H)$  and  $a(H)$  are calculated as a function of  $H$ . Table 1 lists the so-obtained values of  $J_{p0}(H)$  and  $a(H)$  for a broad sequence of applied field strengths, up to  $H_{\max} = 5$  kA/m. We introduce them in the previous equation and we obtain the dependence of the sample polarization  $J_p(w)$  on the strip width at any chosen  $H$  value, as shown in Fig. 2 (solid lines). It is thus observed that the calculated curves excellently predict the experimental  $J_p(w)$  values (symbols), derived from the ensemble of magnetization curves shown in Fig. 1. The vertical dashed line in Fig. 2 provides an estimate for the width  $2L_c$  of the damaged lateral region. We make here an obvious simplification, where we neglect the blur accompanying the transition from the damaged to the undamaged regions. Looking at Fig. 2, we realize that  $2L_c$  must be lower than 5 mm, the minimum investigated strip width (the experimental  $J_p(w)$  is still decreasing). At the same

magnetization curves, no more affected by cutting, coalesce, independent of strip width (see Fig. 1). The  $J_p(w)$  curve calculated for  $H = 5$  kA/m in Fig. 2 (the uppermost curve) must then be a constant quantity across all the  $w$  values, down to  $w = 2L_c$ . We can therefore confidently identify  $2L_c$  with the coordinate in Fig. 2 where such a curve starts to decrease and falls into the forbidden region. We estimate in the present case  $2L_c \sim 3.5$  mm. The peak polarization value pertaining to the damaged region is correspondingly identified, for any  $H$  value, by the intersection of the line  $w = 2L_c$ , with the theoretical  $J_p(w)$  curves. By bringing then Eq. (1) to the limits  $w = 2L_c$  and  $w = \infty$ , we can eventually predict the limiting curves corresponding to the fully work-hardened and the stress-free material, respectively.

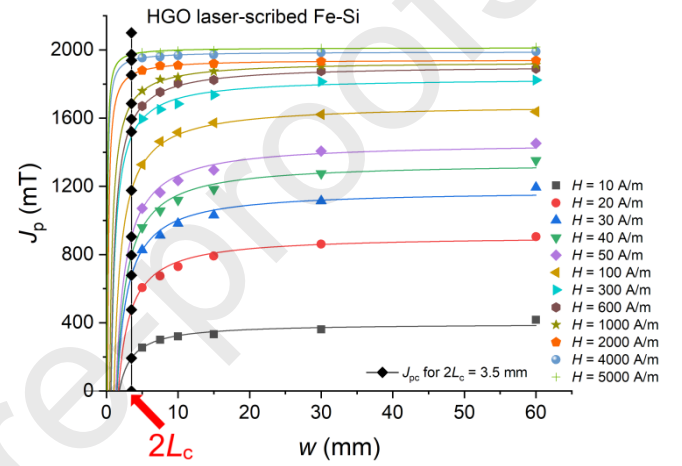


Fig. 2. Magnetic polarization  $J_p$  (symbols), measured at different field strengths in the 0.27 mm HGO Fe-Si samples, as a function of strip width  $w$ . The solid lines are predicted by the hyperbolic function (1). The vertical dashed line identifies the estimated width  $w = 2L_c$  of the fully damaged strip.

Table 1. Behavior of the quantities  $a$ ,  $J_{p0}$  and  $J_{pc}$  provided by Eq. (1) for different values of the applied field  $H$ .

$H$ (A/m)	$a$ (T·m)	$J_{p0}$ (mT)	$J_{pc}$ (mT)
10	0.0007	395.5	193.2
20	0.0015	909.8	476.5
30	0.0017	1177.2	678.1
40	0.0019	1340.3	796.5
50	0.0019	1456.7	905.3
100	0.0017	1680.3	1176.5
200	0.0013	1790.7	1392.3
300	0.0012	1835.7	1492.4
400	0.0012	1875.3	1520.2
500	0.0012	1892.2	1544.7
600	0.0011	1909.02	1569.1
700	0.0011	1922.8	1594.8
800	0.00105	1926.8	1624.7
1000	0.00086	1931.6	1685.9
1500	0.00051	1938.2	1790.3
2000	0.00031	1942.7	1852.7
3000	0.00021	1964.4	1902.8
4000	0.00017	1988.7	1938.2
5000	0.00013	2013.02	1993.7

### 3.2. The hysteresis energy loss

The hysteresis energy loss  $W_h$ , the quantity experimentally obtained by extrapolating the  $W(f)$  curves to  $f \rightarrow 0$ , descends from the dissipation mechanisms related to the fast discontinuities of the domain wall motion (Barkhausen

Following the previous schematic model of the cut strip, we describe, in analogy with Eq. (1), the quasi-static loss  $W_h(w, J_p)$  per unit volume as the weighted sum of the contributions per unit volume  $W_{h0}$  and  $W_{hc}$  associated with the damaged and undamaged slabs, respectively

$$W_h(w, J_p) = W_{h0}(J_{p0}) + (W_{hc}(J_{pc}) - W_{h0}(J_{p0})) \frac{2L_c}{w}, \quad (w \geq 2L_c) \quad (2)$$

where  $W_{hc} \geq W_{h0}$  and the strain-hardened width  $2L_c$  is already known from the previous analysis of the magnetization curves. We consider again the two previous reference strip widths  $w_1$  and  $w_2$  and the related  $W_h(w_1, J_p(H_p))$  and  $W_h(w_2, J_p(H_p))$  experimental behaviors. For any given  $H_p$  value we write Eq. (2) as

$$W_h(w_1, J_{p1}(H_p)) = a_1 + b_1 \left( \frac{2L_c}{w_1} \right) \quad (3a)$$

$$W_h(w_2, J_{p2}(H_p)) = a_1 + b_1 \left( \frac{2L_c}{w_2} \right), \quad (3b)$$

account being taken of the fact that,  $J_{p0}$  and  $J_{pc}$  (hence  $W_{h0}(J_{p0})$  and  $W_{hc}(J_{pc})$ ) are uniquely with known  $H_p$  value. This permits us to determine by Eq. (2)  $W_{h0}(J_{p0})$  and  $W_{hc}(J_{pc})$  for any defined  $w$  and  $J_p$  values. We can thus obtain the hyperbolic  $W_h(w)$  behavior for any  $J_p$  as the volume-weighted sum of  $W_{h0}(J_{p0})$  and  $W_{hc}(J_{pc})$ . This is shown, for  $J_p = 1000$  mT and 1700 mT in Fig. 3, while the individual contributions by the pristine and strain-hardened regions are given in Table 2.

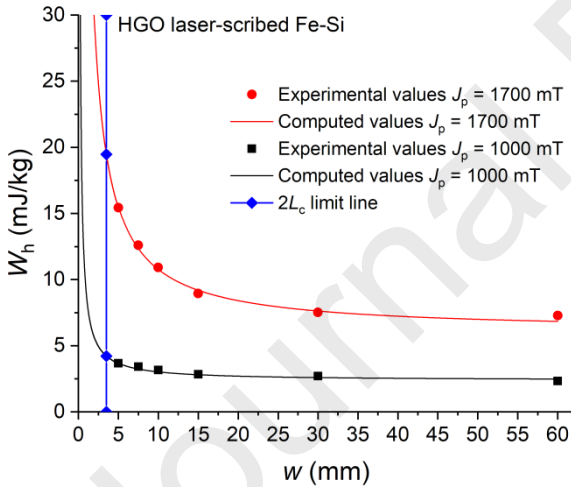


Fig. 3. Hysteresis energy loss  $W_h$  as a function of strip width  $w$  measured at  $J_p = 1000$  mT and 1700 mT (symbols) and their prediction by Eq. (2) (solid lines). The lower limiting width  $w = 2L_c$  of the fully damaged material is signaled by the blue line.

Table 2. Computed values of  $W_{hc}$  and  $W_{h0}$ .

$J_p$ (mT)	$W_{hc}$ (mJ/kg)	$W_{h0}$ (mJ/kg)
1000	4.216	2.378
1700	19.464	6.057

### 3.3. Classical and excess energy losses

The statistical theory of losses [1] was applied to the analysis of the behavior of the measured  $W(f)$  up to 1000 Hz. Fig. 4 illustrates such a behavior for  $J_p = 1000$  mT and 1700 mT and the strip width  $w$  ranging between 5 and 60 mm.

$W_{cl}(f)$ . This is associated with the macroscopic eddy current patterns, whose density increases from the sheet midplane to the surface according to a square law. Since the patterns are concentrated near to and at the surface, we conclude that  $W_{cl}(f)$  is basically related to the flux derivative across the whole cross-section, that is, the average polarization  $J_p$ . It is additionally assumed that plastic straining does not affect the electrical resistivity. It is expected, however, that in the upper frequency range, beyond about 400 Hz, the flux penetration will be incomplete. Under such circumstances, the calculation of  $W_{cl}(f)$  poses certain challenges in GO sheets [20]. We can approximately cope with this problem, provided the skin depth is not far from the specimen half-thickness (0.135 mm in the present case) by ignoring magnetic saturation and assuming an appropriate value  $\mu(J_p)$  for the permeability, according to the standard formulation:

$$W_{cl}(f) = \frac{\pi}{2} \frac{\gamma J_p^2}{\mu} \frac{\sinh \gamma - \sin \gamma}{\cosh \gamma - \cos \gamma}, \quad [\text{J/m}^3] \quad (4)$$

where  $\gamma = \sqrt{\pi \sigma \mu d^2 f}$ ,  $\sigma$  is the conductivity and  $d$  is the sheet thickness [17]. We note that below  $f = 400$  Hz,  $\gamma$  is low enough for Eq. (4) to reduce, once the material density  $\delta$  is introduced, to

$$W_{cl}(f) = \frac{\pi^2}{6} \frac{\sigma d^2 J_p^2}{\delta} f. \quad [\text{J/kg}] \quad (5)$$

Having calculated  $W_h$  and  $W_{cl}(f)$ , we remain with the excess loss

$$W_{exc}(f) = W(f) - W_h - W_{cl}(f), \quad (6)$$

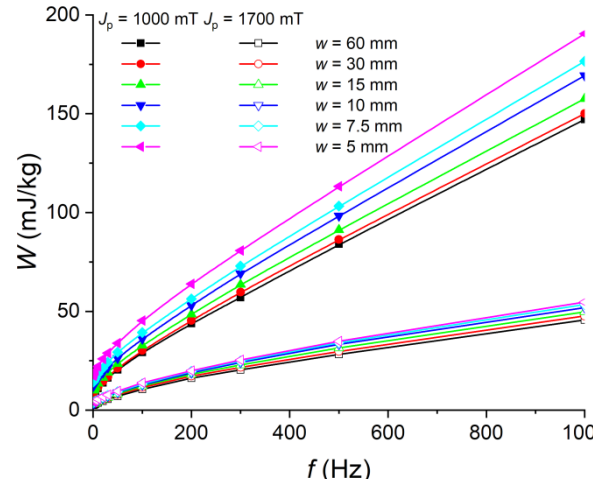


Fig. 4. Energy loss  $W(f)$  measured versus frequency at  $J_p = 1000$  mT and 1700 mT in punched 0.27 mm thick HGO Fe-Si strips. The strip width ranges between 5 and 60 mm.

that is, the extra dynamic loss engendered by the motion of the domain walls. The HGO sheets exhibit a wide domain spacing and  $W_{exc}(f)$  can provide the largest contribution to  $W(f)$  at power frequencies. The  $W_{exc}(f)$  curves extracted from  $W(f)$  using Eq. (6) are shown in Fig. 5. They follow an  $f^{1/2}$  dependence and display an increasing trend under decreasing strip width, emulating to some extent the behavior of  $W_h$ . This is not surprising, because it is exactly what is predicted

b) application to the theory of excess losses [19].

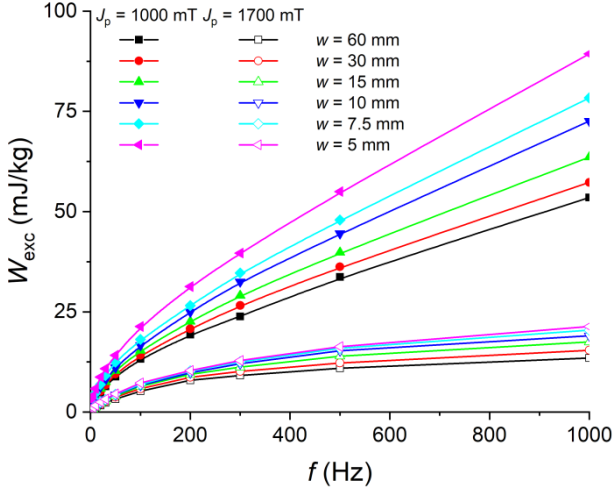


Fig. 5. Excess energy loss  $W_{\text{exc}}(f)$  versus frequency at  $J_p = 1000$  mT and 1700 mT in punched 0.27 mm thick HGO Fe-Si strips. The excess loss component  $W_{\text{exc}}(f)$  is extracted from  $W(f)$  according to Eq. (6).

$W_{\text{exc}}(f)$  is associated with the eddy currents circulating in the neighborhood of the domain walls. The mesoscopic character of these currents makes it possible to distinguish between the contributions to  $W_{\text{exc}}(f)$  provided by the strain-hardened bands and the pristine core of the strip. This permits us to adopt the very same approach followed with the hysteresis loss and write at any frequency

$$W_{\text{exc}}(w, J_p, f) = W_{\text{exc}0}(J_{p0}, f) + \left( W_{\text{exc}c}(J_{pc}, f) - W_{\text{exc}0}(J_{p0}, f) \right) \frac{2L_c}{w}, \quad (7)$$

with  $W_{\text{exc}0}(J_{p0}, f)$  and  $W_{\text{exc}c}(J_{pc}, f)$  pertaining to the middle and the lateral bands, respectively. We shall consider again the experimental  $W_{\text{exc}}(f)$  measured on the reference widths  $w_1$  and  $w_2$  and we shall repeat, for any selected frequency, the procedure previously devised for the determination of  $W_{h0}(J_{p0})$  and  $W_{hc}(J_{pc})$  versus  $w$  and  $J_p$ . Consequently, we arrive at predicting by Eq. (7)  $W_{\text{exc}}$  versus  $w$ , as shown, for selected frequency values and  $J_p = 1000$  mT and 1700 mT, in Fig. 6.

As predicted by the theory, the increase of coercivity and hysteresis loss by mechanical hardening is attended by parallel, though somewhat mitigated, increase of the excess losses. The specific values  $W_{\text{exc}0}(J_{p0}, f)$  and  $W_{\text{exc}c}(J_{pc}, f)$  found at  $f = 50$  Hz for the two investigated polarization levels  $J_p = 1000$  mT and 1700 mT are given in Table 3.

It is concluded that the measured loss  $W(f) = W_h + W_{\text{cl}}(f) + W_{\text{exc}}(f)$  can be remarkably affected by mechanical cutting already at power frequencies, thanks to the increase by strain hardening of  $W_h(f)$  and  $W_{\text{exc}}(f)$ . By the theoretical formulation one can predict, in particular, that around 13 % increase of  $W(f)$  at 50 Hz and 1.7 T peak polarization is engendered in standard 30 mm wide Epstein strips.

Table 3. Computed values at 50 Hz of the two contributions  $W_{\text{exc}c}$  and  $W_{\text{exc}0}$  for the polarization levels  $J_p = 1000$  mT and 1700 mT

$J_p$ (mT)	$W_{\text{exc}c}$ (mJ/kg)	$W_{\text{exc}0}$ (mJ/kg)
1000	5.016	3.458
1700	16.586	8.453

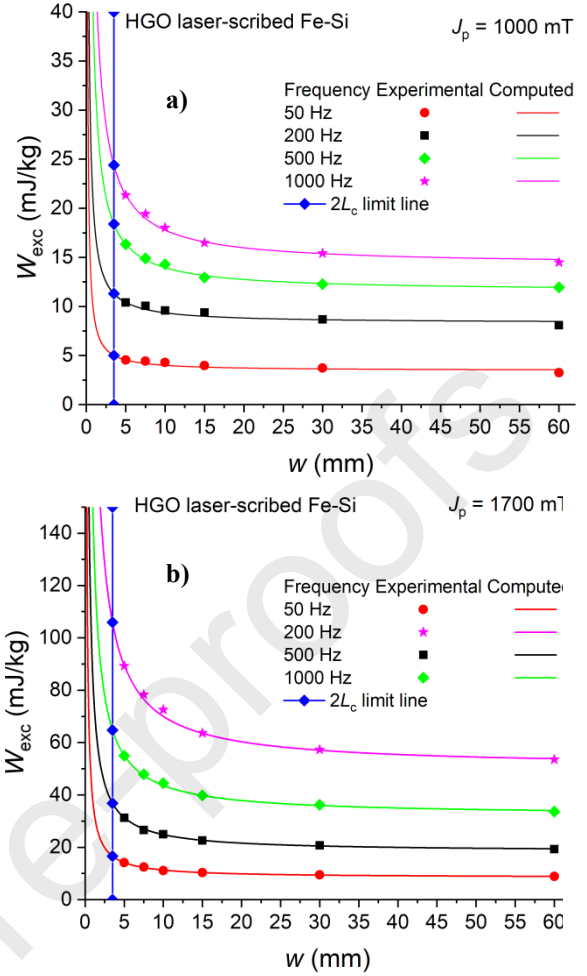


Fig. 6. Excess loss  $W_{\text{exc}}$  versus strip width in the punched 0.27 mm thick HGO Fe-Si strips. Solid lines and symbols refer to Eq. (7) and the experiments, respectively. Selected frequency values at  $J_p = 1000$  mT (a) and 1700 mT (b) are considered. The intercepts of the vertical line with the  $W_{\text{exc}}(w)$  curves provide the excess loss values pertaining to the  $2L_c$  wide fully strain-hardened bands.

#### 4. Conclusions

We have investigated the effect of mechanical cutting on the magnetization curve and energy loss of HGO Fe-Si steel sheets, by measurements on guillotine-punched strips of widths 60 to 5 mm between 1 Hz and 1000 Hz. A simple geometrical model, where the tested strip is composed of an unscathed core and two strain-hardened lateral bands permits one, in association with the loss decomposition procedure, to provide the analytical dependence of the hysteresis  $W_h$  and excess  $W_{\text{exc}}(f)$  losses on the strip width. The formulation provides  $W_h$  and  $W_{\text{exc}}(f)$  in terms of volume-weighted sum of the same quantities pertaining to the stress-free and the strain hardened slabs, respectively. A prediction can then be made of the evolution of  $W_h$  and  $W_{\text{exc}}(f)$  as a function of the strip width, while estimating the breadth of the damaged region at the strip edges. Both loss components are observed to follow the predicted hyperbolic dependence on the strip width  $w$ , with an upper value attained for  $w \cong 3.5$  mm (fully strain-hardened strip). It is concluded that in the unrelieved 30 mm Epstein strips the guillotine cutting leads to an increase around 13 % of the 50 Hz energy loss at 1.7 T.

#### Acknowledgement

Ministry of Education and Research, CCCDI - UEFISCDI, project number PN-III-P2-2.1-PTE-2019-0423 (47PTE/2020), within PNCDI III.

## References

- [1] B. Weidenfeller and M. Anhalt, Effect of laser treatment on high and low induction loss components of grain-oriented iron silicon sheets, *J. Magn. Magn. Mater.* 322 (2010) 69-72. <https://doi.org/10.1016/j.jmmm.2009.08.030>
- [2] P. Rauscher, B. Betz, J. Hauptmann, A. Wetzig, E. Beyer, and C. Grünzweig, The influence of laser scribing on magnetic domain formation in grain-oriented electrical steel visualized by directional neutron dark-field imaging, *Sci. Rep.* 6 (2016) 38307. <https://doi.org/10.1038/srep38307>.
- [3] F. Fiorillo, Advances in Fe-Si properties and their interpretation, *J. Magn. Magn. Mater.* 157-158 (1996) 428-431. [https://doi.org/10.1016/0304-8853\(95\)01244-3](https://doi.org/10.1016/0304-8853(95)01244-3).
- [4] M. Nesser, O. Maloberti, E. Salloum, J. Dupuy, S. Panier, C. Pineau, J.-P. Birat, J. Fortin, and P. Dassonville, Impact of Ultra-Short Pulsed Laser (USPL) Ablation process on Separated loss coefficients of grain oriented electrical steels, *IEEE Trans. Magn.*, 58 (2022) 2001105. <https://doi.org/10.1109/TMAG.2022.3152899>.
- [5] IEC Standard Publication 60404-3, Methods of measurement of the magnetic properties of electrical steel strip and sheet by means of a single sheet tester, Ed. 2.2, IEC Central Office, 2010. <https://webstore.iec.ch>.
- [6] G. Shilyashki, H. Pfützner, M. Gießing, and C. Bengtsson, Giant Epstein tester for magnetic energy loss measurements of non-annealed domain-refined Fe-Si, *IEEE Trans. Magn.*, 58 (2022) 6000606. <https://doi.org/10.1109/TMAG.2022.3158473>.
- [7] A. Kedous-Lebouc, O. Messal, A. Youmssi, Joint punching and frequency effects on practical magnetic characteristics of electrical steels for high-speed machines, *J. Magn. Magn. Mater.* 426 (2017) 658-665. <https://doi.org/10.1016/j.jmmm.2016.10.150>.
- [8] P. Baudouin, M. D. Wulf, L. Kestens, and Y. Houbaert, The effect of the guillotine clearance on the magnetic properties of electrical steels, *J. Magn. Magn. Mater.*, 256 (2003) 32 – 40. [https://doi.org/10.1016/S0304-8853\(02\)00004-5](https://doi.org/10.1016/S0304-8853(02)00004-5).
- [9] G. Crevecoeur, P. Sergeant, L. Dupre, L. Vandenbossche, and R. V. de Walle, Analysis of the local material degradation near cutting edges of electrical steel sheets, *IEEE Trans. Magn.*, 44 (2008) 3173–3176. <https://doi.org/10.1109/TMAG.2008.2001605>.
- [10] S. Steentjes, G. von Pfingsten, and K. Hameyer, An application-oriented approach for consideration of material degradation effects due to cutting on iron losses and magnetizability, *IEEE Trans. Magn.*, 50 (2014) 7027804. <https://doi.org/10.1016/j.jmmm.2015.08.010>.
- [11] M. Hofmann, H. Naumoski, U. Herr, and H. Herzog, Magnetic properties of electrical steel sheets in respect of cutting: Micromagnetic analysis and macromagnetic modeling, *IEEE Trans. Magn.*, 52 (2016) 2000114. <https://doi.org/10.1109/TMAG.2015.2484280>.
- [12] M. Bali and A. Muetze, Modeling the effect of cutting on the magnetic properties of electrical steel sheets, *IEEE Trans. Ind. Electron.*, 64 (2017) 2547–2556. <https://doi.org/10.1109/TIE.2016.2589920>.
- [13] H. Zhao, E. Ferrara, V. Manescu (Paltanea), G. Paltanea, H. Gavrilă, F. Fiorillo, Effect of punching and water-jet cutting methods on magnetization curve and energy losses of non-oriented magnetic steel sheets, *Int. J. Appl. Electrom.* 55 (2017) 69-76. <https://doi.org/10.3233/JAE-172259>
- [14] V. Manescu (Paltanea), G. Paltanea, E. Ferrara, I.V. Nemoianu, F. Fiorillo, H. Gavrilă, Influence of mechanical and water-jet cutting on the dynamic magnetic properties of NO Fe-Si steels, *J. Magn. Magn. Mater.* 499 (2020) 166257. <https://doi.org/10.1016/j.jmmm.2019.166257>.
- [15] V. Manescu (Paltanea), G. Paltanea, H. Gavrilă, Non-oriented silicon iron alloys – State of the art and challenges, *Rev. Roum. Sci. Techn. – Série Électrotechnique et Énergétique*, 59, 4, (2014) 371-380.
- [16] G. Paltanea, V. Manescu - Paltanea, H. Gavrilă, A. Nicolaide, B. Dumitrescu, Comparison between magnetic industrial frequency properties of non-oriented FeSi alloys, cut by mechanical and water jet technologies, *Rev. Roum. Sci. Techn. – Série Électrotechnique et Énergétique* 61 (2016) 26-31.
- [17] V. Manescu-Paltanea, G. Paltanea, I.V. Nemoianu, Degradation of static and dynamic magnetic properties of non-oriented steel sheets <https://doi.org/10.1109/TMAG.2018.2834375>.
- [18] G. Paltanea, V. Paltanea, I.V. Nemoianu, Magnetic properties of non-oriented silicon iron sheets in case of external applied thermal treatments, *Rev. Roum. Sci. Techn. – Série Électrotechnique et Énergétique*, 55, 4, (2010) 357-364.
- [19] G. Bertotti, *Hysteresis in magnetism*, Academic Press, 1998, p. 404.
- [20] A. Magni, A. Sola, O. de la Barrière, E. Ferrara, L. Martino, C. Ragusa, C. Appino, and F. Fiorillo, Domain structure and energy losses up to 10 kHz in grain-oriented Fe-Si sheets, *AIP Adv.*, 11 (2021) 015220. <https://doi.org/10.1063/9.0000184> (2021).

## Highlights

1. Simple phenomenological model regarding the dependence of energy losses on the strip width
2. Simple phenomenological model regarding the dependence of magnetization curve on the strip width
3. Energy loss separation
4. Estimation of cutting damaged width strip

## Declaration of interests

The authors declare that they have no known competing financial interests or personal relationships that could have appeared to influence the work reported in this paper.

The authors declare the following financial interests/personal relationships which may be considered as potential competing interests: